Influence of External Current on Yokeless Electric Current Transducers

Pavel Ripka and Andrey Chirtsov

Faculty of Electrical Engineering, Czech Technical University, 16627 Prague, Czech Republic

Yokeless electric current transducers have compact size, but they are sensitive to external magnetic fields, including those caused by electric currents in their vicinity. It is often believed that this unwanted sensitivity can be effectively suppressed by using a differential sensor. In this paper, we investigate the effect of external current with arbitrary position on busbar differential current sensor. We show the main disadvantage of the differential current sensor: increased sensitivity to currents in the transversal direction, which are not sensed by a single sensor. We analyze by finite element method simulation also the influence of real conductor size and uneven density of ac currents. The results were verified on 1000 A current transducer using a pair of microfluxgate sensors. The realistic suppression of close currents depends on the conductor angular position and in 10 cm distance it can be as low as 50, but it can be corrected if the geometry is known.

Index Terms— **Current sensor, fluxgate, Hall sensor, microfluxgate.**

I. Introduction

CONTACTLESS transducers of dc electric currents often have magnetic yoke, which concentrates the flux generated by the measured current. As a result, the reading does not depend much on the conductor position inside the magnetic circuit. The yoke also shields against external magnetic fields, including those caused by external currents (crosstalk error) [1]. Hall sensors, which are slim in the measuring direction, fit into the narrow airgap in the yoke and therefore dominate in this application. Other transducers of this type have a small fluxgate sensor in the slot of the yoke, or the whole yoke is ac excited and works as fluxgate sensor [2], [3]. Closed-loop current transducers with yoke easily achieve accuracy below 0.1%. However, for many applications the open-loop configuration is used, which is less power consuming and low cost. Sensitivity drift of the Hall sensor can be compensated using microsystem with autocalibration coil [4] down to 80 ppm/K.

However, for large currents and high-voltage networks, the yoke becomes too large and heavy to prevent saturation and ensure the required distance from the high-voltage conductor. In these cases, the yokeless solution is required. The important advantage of yokeless current sensor is the absence of ferromagnetic material, which can be saturated by overcurrent [5]. The integrated yokeless current sensors have limited current range: 5 A sensor of this type is described in [6]. Commercially available yokeless high-current transducers use discrete sensors on both sides of the bus bar [7]. This configuration has main disadvantages as follows.

1) Magnetic field on the surface of the conductor is large so that precise magnetic sensors, such as magnetoresistors or fluxgates, cannot be used.
2) Busbar movement or uneven current distribution in the busbar causes measurement error.
3) Suppression of the external currents by gradiometric sensor is low, as the sensor distance is high. Later, in this paper, we derive formula proving this claim for the arbitrary position of the external conductor.

George suggested to suppress the influence of the measured conductor position by calculating $B_1 \times B_2/(B_1+B_2)$ [8]. However, this trick would destroy the immunity of the differential transducer against external currents.

Chen and Chen [9] used four Hall sensors on each conductor and measured errors caused by external currents. They found that the difference between calculated and measured errors was below 6% for conductors in the close vicinity, and this difference is rapidly decreasing with an increase in distance between conductors.

Circular sensor array with more than four sensors around the conductor approximates better the closed line integral in Ampere's law. This brings better immunity against the position of the measured conductor [10] as well as against the crosstalk from external conductors [11]. Both errors decrease with an increasing number of sensors; eight sensors are considered as an optimum number. Further, error reduction can be achieved by using crosstalk reduction algorithm, but this is impractical for industrial applications because of the large computational complexity of the necessary non-linear solver. Circular sensor array still limits the maximum measurable current when using precise magnetic sensors. For 100 mm diameter array, the maximum measurable current is 50 A for anisotropic magnetoresistive sensors (AMR) and 500 A for microfluxgate sensor, taking into account their field range of 0.2 and 2 mT, respectively.

In this paper, we analyze the influence of the external current on the differential current transducer. We start with the analytical calculation of the influence of the idealized current, follow with Finite Element Method (FEM) simulation of the real conductor, including the effects of the eddy currents and finish by the experimental verification of selected configurations.

II. Bussbar Transducer for High Currents

Mounting a differential magnetic field sensor inside the busbar solves the problem with limited range as the sensitivity

Manuscript received March 10, 2017; revised April 13, 2017; accepted June 2, 2017. Date of publication June 13, 2017; date of current version October 24, 2017. Corresponding author: P. Ripka (e-mail: ripka@fel.cvut.cz).

Color versions of one or more of the figures in this paper are available online at http://ieeexplore.ieee.org.

Digital Object Identifier 10.1109/TMAG.2017.2715075

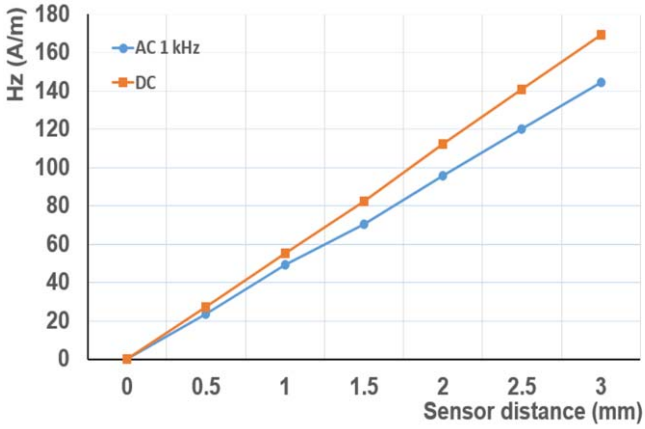

Fig. 1. Sensitivity s as a function of the sensor gradiometric distance 2a (FEM simulation) for dc and 1 kHz.

s and thus the current range can be adjusted by the sensor distance from the center of symmetry [12]. External currents are suppressed by measuring the field gradient using a pair of sensors.

For all measurements in this paper, we have used DRV425 microfluxgate sensors [13]. These sensors have very low offset tempco of 5 nT/K, which makes them superior to other room-temperature miniature magnetic sensors such as Hall (5 μT/K is typical value for commercially available devices such as Infenion TLE 4997) or any type of magnetoresistors (241 nT/K for KMZ 51). They also have low crossfield error below 10 nT [14], which results in excellent linearity for the uncompensated sensor.

In our case, the differential microfluxgate sensors are inserted into the cylindrical 19 mm hole in the 60 × 10 mm copper busbar. For the sensor distance of 2a = 2.5 mm, the sensitivity to the dc-measured current calculated by FEM is $s = 2$ (A/m)/A, and this value was also verified experimentally. For ac currents, the current density is no longer homogeneous because of the eddy currents, and the sensitivity drops down with frequency. Fig. 1 shows the calculated sensitivity as a function of sensor distance for dc-measured current and also for ac-measured current with $f = 1$ kHz. Decreasing sensor distance generally reduces crosstalk error, but the effective suppression factor is even getting worse due to the decreased sensitivity s to the measured field.

III. Lateral External Current

Parasitic response to the external current can be analytically calculated only for the simplified case when the current is localized to one point. For the differential sensor with spacing (base) of 2a, the parasitic response to the idealized external current I in the distance of d in the same plane is

$$H_1 - H_3 = I\frac{a}{\pi(d+2a)d}. \quad (1)$$

Response to the realistic external in-plane current bar with dc current of 100 A was modeled by FEM. The result of such simulation for a single sensor is shown in Fig. 2(a) and for the differential sensor is shown in Fig. 2(b). The simulated values

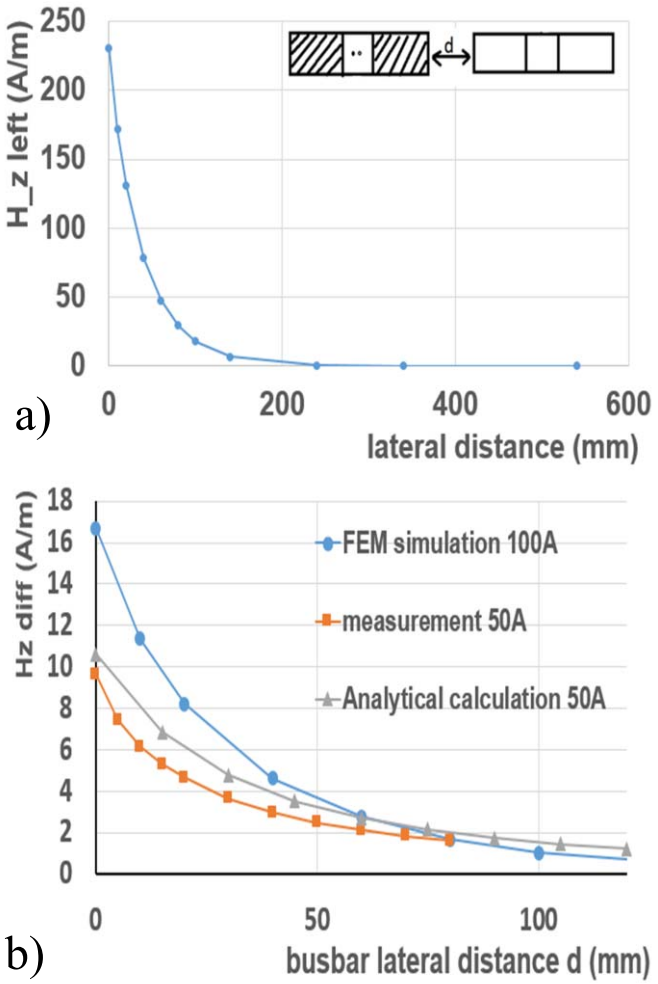

Fig. 2. Response to external lateral 100 A dc current as a function of distance between the busbars. (a) FEM-calculated single sensor. (b) Differential sensor: FEM-calculated simulation for 100 A dc current (upper trace), analytical calculation (middle trace), and measurement for 50 A current (lower trace).

for differential sensor are also compared to the measured values and values calculated using (1).

For our selected geometry, the external current in a 9 cm distant busbar is suppressed only by the factor of 66. Compared to the circular array of eight sensors, which for the same distance has a suppression of 250, the crosstalk error is still high.

IV. Superior External Current

The less known fact is that if the external current is outside the plane, the situation is not much better. If the external current I is in the perpendicular plane, the gradiometer does not suppress it any more. The simplified situation is illustrated in Fig. 3: sensors 1 and 3 measure field from two halves of busbar sensor current I_m. This current creates field components H_{1m} and H_{3m} in the sensitive axes of the two sensors. The idealized localized external field I in the distance d creates fields H_1 and H_3 from which the sensors measure their H_{1y} and H_{3y} components. The parasitic response is similar to the

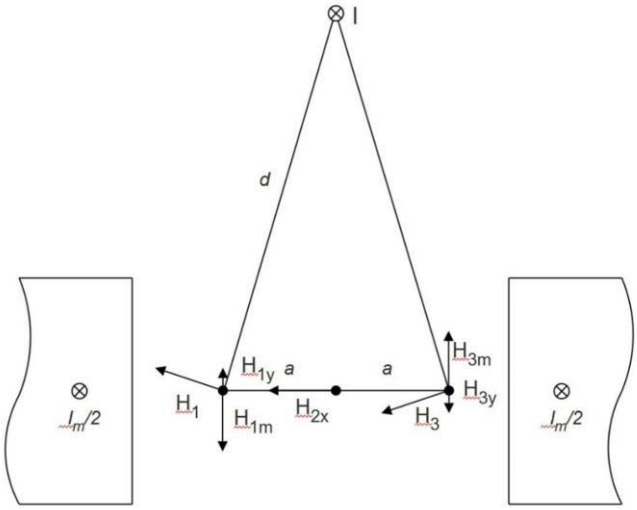

Fig. 3. Magnetic field components in points 1 and 2 where the two sensors are located. These sensors measure field in the y-direction.

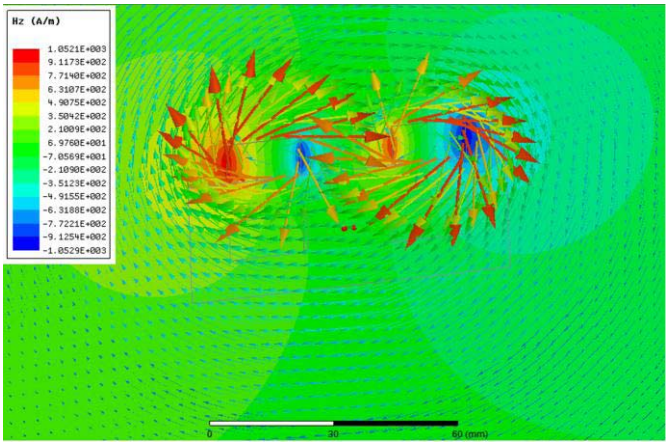

Fig. 4. Field vector image for external busbar in superior position in 10 mm distance from the measuring busbar.

previous case

$$H_{1y} - H_{3y} = I\frac{a}{\pi d^2}. \tag{2}$$

A. Real Conductors: DC Case

For the real conductors, the current is homogeneously distributed in the external busbar, and the field map is shown in Fig. 4.

The parasitic response for dc superior current is shown in Fig. 5. The shape of the characteristics in the close vicinity of the busbars is complicated, but for practical applications, this case is not realistic. For larger distances, the characteristics approximate the analytically calculated monotonous dependence.

B. AC Case

If the external current is alternating, the situation is complicated by the influence of the eddy currents: the current

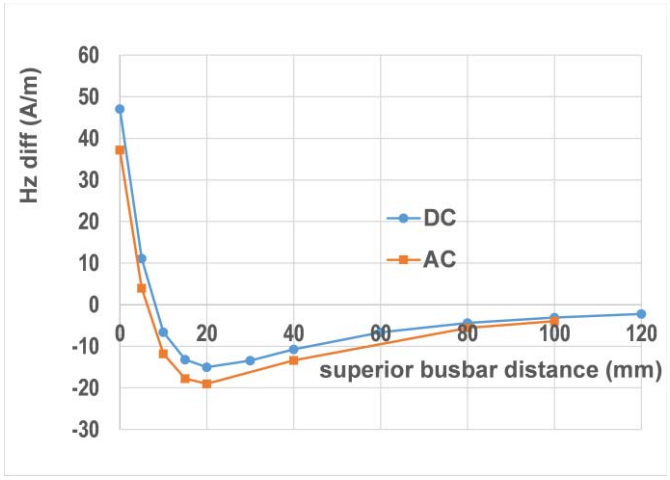

Fig. 5. Response to external superior 100 A dc current as a function of a distance between the busbars (FEM simulation).

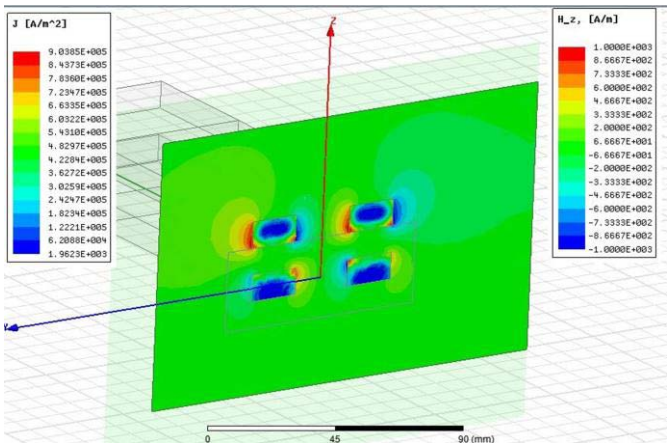

Fig. 6. AC case: current and field distribution for external busbar in superior position in 10 mm distance from the measuring busbar.

density in the external busbar is not uniform, and the external current also induces eddy currents in the measured conductor. Fig. 6 shows an example of current and field distributions for external current of 100 A/1 kHz. However, the FEM calculated response in larger distances is not different from the dc case.

V. External Current in Arbitrary Position

Fig. 7(a) illustrates the general case when the external field I is declined by an angle φ from the sensor line. The field was calculated for $d = 0.1$ m, $I = 100$ A, and $a = 0.00125$ m. The field difference caused by the idealized external current I can be again easily calculated analytically

$$H_{1y} - H_{3y} = I\left(\frac{\cos\varphi_1}{r_1} - \frac{cos\varphi_3}{r_3}\right), \tag{3}$$

where

$$\begin{aligned} \varphi_1 &= \operatorname{arctg}\tfrac{r\cdot\sin\varphi}{r\cdot\cos\varphi+a}; \\ \varphi_3 &= \operatorname{arctg}\tfrac{r\cdot\sin\varphi}{r\cdot\cos\varphi-a}; \\ r_{1,3} &= \tfrac{r\sin\varphi}{\sin\varphi_{1,3}}. \end{aligned}$$

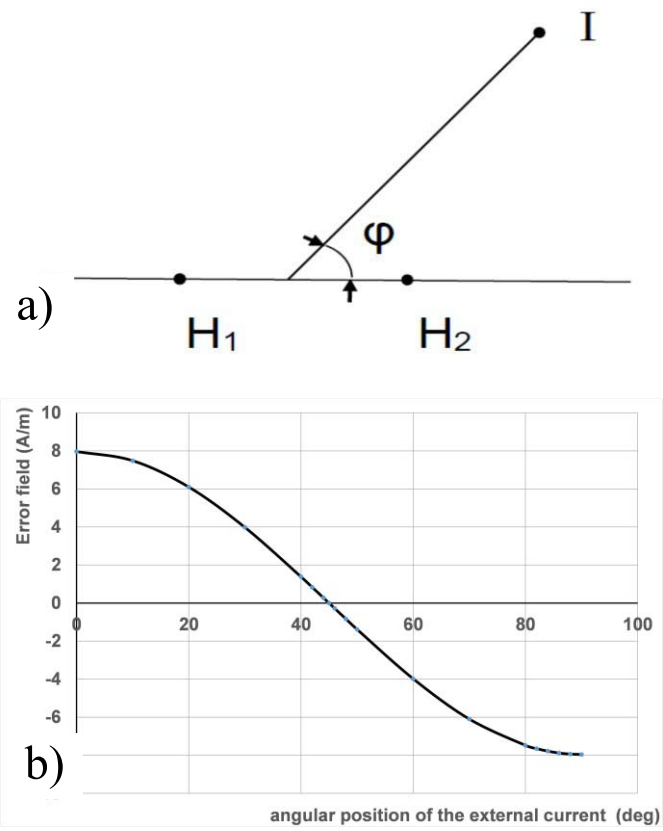

Fig. 7. External current I in arbitrary angular position. (a) Definition of the position angle. (b) Error field as a function of angular position of an idealized $I = 1000$ A in a distance of 0.1 m.

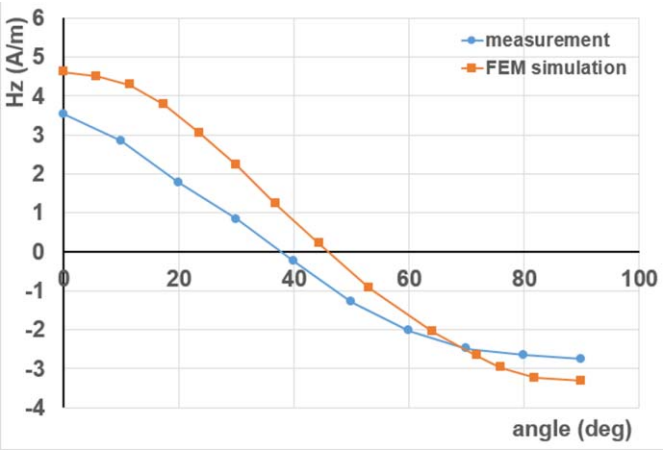

Fig. 8. Response to external dc current in busbar in arbitrary position: FEM simulation and measurement. Distance between the centers of busbars was 100 mm, which corresponds to 40 mm distance between busbars.

The calculated values from (3) are shown in Fig. 7(b), and the result of simulations together with the measured response is shown in Fig. 8. It is clear that (3) can be used only for large distances between the busbars.

VI. Conclusion

External current has significant influence on the reading of the yokeless current transducer. Circular transducers with typically eight sensors present the solution with the best crosscurrent suppression. However, for 10 cm diameter, their range is limited by Ampere's law to 50 A for AMR and 500 A for microfluxgate sensors. Hall sensors can be used to increase the measuring range but only for ac currents, as their dc drift is 1000-times higher compared to microfluxgate sensors.

A transducer with a differential fluxgate sensor inside the busbar can overcome this limitation; however, its sensitivity to external currents is high. We show that this unwanted sensitivity depends on the angular position in a more complex way than it was generally believed. The response reaches minimum for the angle of 45°, and for larger angles, it increases again. The response to external currents depends only on the frequency in very small distances.

If the position of the external conductor is fixed (such as in three-phase systems or switchboards) and all the currents are measured, compensation of the cross-sensitivity can be calculated based on the calculated cross-sensitivity parameters.

Acknowledgment

This work was supported by the Grant Agency of the Czech Republic through the project "New Methods for the Measurement of Electric Currents" under Grant GACR 17-19877S. The work of A. Chirtsov was supported by Texas Instruments academic grant.

References

[1] P. Ripka, "Electric current sensors: A review," *Meas. Sci. Technol.*, vol. 21, no. 11, pp. 1–23, 2010.

[2] P. Ripka, K. Draxler, and R. Styblikova, "AC/DC current transformer with single winding," *IEEE Trans. Magn.*, vol. 50, no. 4, Apr. 2004, Art. no. 8400504.

[3] X. Yang, Y. Li, W. Zheng, W. Guo, Y. Wang, and R. Yan, "Design and realization of a novel compact fluxgate current sensor," *IEEE Trans. Magn.*, vol. 51, no, 3, Mar. 2015, Art. no. 4002804.

[4] A. Ajbl, M. Pastre, and M. Kayal, "A fully integrated Hall sensor microsystem for contactless current measurement," *IEEE Sensors J.*, vol. 13, no. 6, pp. 2271–2278, Jun. 2013, doi: 10.1109/JSEN.2013.2251971.

[5] Y.-P. Tsai, K.-L. Chen, Y.-R. Chen, and N. Chen, "Multifunctional coreless hall-effect current transformer for the protection and measurement of power systems," *IEEE Trans. Magn.*, vol. 63, no. 3, pp. 557–565, Mar. 2014.

[6] V. Frick, L. Hebrard, P. Poure, F. Anstotz, and F. Braun, "CMOS microsystem for AC current measurement with galvanic isolation," *IEEE Sensors J.*, vol. 3, no. 6, pp. 752–760, Dec. 2003.

[7] M. Blagojević, U. Jovanović, I. Jovanović, D. Mančić, and R. S. Popović, "Realization and optimization of bus bar current transducers based on Hall effect sensors," *Meas. Sci. Technol.*, vol. 27, no. 6, p. 065102, 2016.

[8] N. George and S. Gopalakrishna, "An improved anti-differential configuration based Hall-effect current sensor," in *Proc. IEEE Annu. India Conf. (INDICON)*, Bangalore, India, Dec. 2016, pp. 1–5.

[9] K.-L. Chen and N. Chen, "A new method for power current measurement using a coreless Hall effect current transformer," *IEEE Trans. Instrum. Meas.*, vol. 60, no. 1, pp. 158–169, Jan. 2001.

[10] P. Mlejnek, M. Vopalensky, and P. Ripka, "AMR current measurement device," *Sens. Actuators A, Phys.*, vol. 141, no. 2, pp. 649–653, 2008.

[11] L. D. Rienzo and Z. Zhang, "Spatial harmonic expansion for use with magnetic sensor arrays," *IEEE Trans. Magn.*, vol. 46, no. 1, pp. 53–58, Jan. 2010.

[12] P. Ripka, M. Přibil, V. Petrucha, V. Grim, and K. Draxler, "A fluxgate current sensor with an amphitheater busbar," *IEEE Trans. Magn.*, vol. 52, no. 7, Jun. 2016, Art. no. 4002004.

[13] M. F. Snoeij, V. Schaffer, S. Udayashankar, and M. V. Ivanov:, "Integrated fluxgate magnetometer for use in isolated current sensing," *IEEE J. Solid-State Circuits*, vol. 51, no. 7, pp. 1684–1694, Jul. 2016.

[14] P. Ripka, M. Janosek, M. Butta, S. W. Billingsley, and E. Wakefield, "Crossfield error in fluxgate and AMR sensors," *J. Electr. Eng.*, vol. 61, pp. 13–16, Jun. 2010.